

RESEARCH ARTICLE

In vivo experiments demonstrate the potent antileishmanial efficacy of repurposed suramin in visceral leishmaniasis

Supriya Khanra¹, Subir Kumar Juin², Junaid Jibran Jawed³, Sweta Ghosh², Shreyasi Dutta⁴, Shaik Abdul Nabi⁵, Jyotirmayee Dash⁶, Dipak Dasgupta⁴, Subrata Majumdar^{2*}, Rahul Banerjee^{1,7*}

1 Crystallography and Molecular Biology Division, Saha Institute of Nuclear Physics, Bidhannagar, Kolkata, India, **2** Division of Molecular Medicine, Bose Institute, Kolkata, India, **3** School of Biotechnology, Department of Life Sciences, Presidency University-New Campus, Kolkata, India, **4** Biophysics and Structural Genomics Division, Saha Institute of Nuclear Physics, Bidhannagar, Kolkata, India, **5** Department of Medicinal Chemistry, National Institute of Pharmaceutical Education and Research, Kolkata, India, **6** Department of Organic Chemistry, Indian Association for the Cultivation of Science, Jadavpur, Kolkata, India, **7** HomiBhabha National Institute, Anushakti Nagar, Mumbai, India

* subrata@jcbose.ac.in (SM); rahul.banerjee@saha.ac.in (RB)



OPEN ACCESS

Citation: Khanra S, Juin SK, Jawed JJ, Ghosh S, Dutta S, Nabi SA, et al. (2020) *In vivo* experiments demonstrate the potent antileishmanial efficacy of repurposed suramin in visceral leishmaniasis. PLoS Negl Trop Dis 14(8): e0008575. <https://doi.org/10.1371/journal.pntd.0008575>

Editor: Abhay R. Satoskar, Ohio State University, UNITED STATES

Received: November 19, 2019

Accepted: July 7, 2020

Published: August 31, 2020

Copyright: © 2020 Khanra et al. This is an open access article distributed under the terms of the [Creative Commons Attribution License](#), which permits unrestricted use, distribution, and reproduction in any medium, provided the original author and source are credited.

Data Availability Statement: All relevant data are within the manuscript and its Supporting Information files.

Funding: The work reported in the manuscript has been supported by the intramural grants from Department of Atomic Energy, Government of India (Projects of SINP:-MSACR [XII-R&D-SIN-5.04-0102]). The funders had no role in study design, data collection and analysis, decision to publish, or preparation of the manuscript.

Abstract

Background

Treatment failure and resistance to the commonly used drugs remains a major obstacle for successful chemotherapy against visceral leishmaniasis (VL). Since the development of novel therapeutics involves exorbitant costs, the effectiveness of the currently available anti-trypanosomatid drug suramin has been investigated as an antileishmanial, specifically for VL, *in vitro* and in animal model experiments.

Methodology/Principal

Leishmania donovani promastigotes were treated with suramin and studies were performed to determine the extent and mode of cell mortality, cell cycle arrest and other *invitropara*-parameters. In addition, *L. donovani* infected BALB/c mice were administered suramin and a host of immunological parameters determined to estimate the antileishmanial potency of the drug. Finally, isothermal titration calorimetry (ITC) and enzymatic assays were used to probe the interaction of the drug with one of its putative targets namely parasitic phosphoglycerate kinase (LmPGK).

Findings

The *in vitro* studies revealed the potential efficacy of suramin against the *Leishmania* parasite. This observation was further substantiated in the *in vivo* murine model, which demonstrated that upon suramin administration, the *Leishmania* infected BALB/c mice were able to reduce the parasitic burden and also generate the host protective immunological responses. ITC and enzyme assays confirmed the binding and consequent inhibition of LmPGK due to the drug.

Competing interests: The authors have declared that no competing interests exist.

Conclusions/Significance

All experiments affirmed the efficacy of suramin against *L. donovani* infection, which could possibly lead to its inclusion in the repertoire of drugs against VL.

Author summary

Visceral Leishmaniasis (VL) or Kala-azar, classed as a neglected tropical disease, is still a major problem worldwide, aggravated by increasing parasitic resistance against the drugs commonly used for its treatment. Since the development of novel therapeutics involves exorbitant costs, the effectiveness of the currently available antitrypanosomatid drug suramin has been investigated as an antileishmanial, specifically for VL, *in vitro* and in animal model experiments. Our study showed that suramin is effective against *L. donovani* and significantly reduced the (splenic/hepatic) parasitic burden in *L. donovani* infected BALB/c mice, switching the immune response in the infected BALB/c mice from T_{H2} to aT_{H1} type. The ITC data confirmed that suramin does indeed interact with parasitic phosphoglycerate kinase (LmPGK) and enzyme assays demonstrated the inhibition of LmPGK due to the drug. Therefore, our investigation raises the possibility of suramin being included in the repertoire of drugs used to treat VL.

Introduction

Visceral Leishmaniasis (VL) or Kala-azar, classed as a neglected tropical disease, afflicts about half a million people worldwide, with over 90% of the cases occurring primarily in the poverty stricken regions of Brazil, Ethiopia, India, Somalia, and Sudan [1]. VL caused by the protozoan parasite *Leishmania donovani*, (transmitted by the phlebotomine sand fly), is almost certainly lethal without timely clinical interventions [2]. The last decade has seen a significant drop in the incidence of VL primarily from India and Bangladesh (due to the widespread use of insecticide treated nets) though the epidemiological status of the disease in other African countries including Brazil continues to be negative [3]. In Brazil VL has gradually spread from predominantly rural areas to densely populated urban centers. Thus, overall the threat to public health by VL remains unabated. The situation is further aggravated by the emergence of Leishmanial strains resistant to antimonial drugs [4], the traditional first line of defence against VL and also their replacements such as amphotericin B and miltefosine [5, 6]. Most of the drugs used to treat VL have severe side effects, can only be administered in hospital settings and are expensive [7]. Therefore, there is an urgent need to identify economically viable and potent antileishmanials.

Previous work in our laboratory had identified the efficacy of the polysulphonatednaphthylamine drug suramin as a potent antileishmanial against *L. donovani* [8]. Currently, suramin is used to treat the hemolymphatic stage of African trypanosomiasis (sleeping sickness) caused by *Trypanosoma brucei rhodesiense* and has been reported to inhibit the glycolytic enzymes of the parasite [9]. Suramin has also shown much promise as a prospective antiviral inhibiting the envelope mediated gene transfer and the replication of chikungunya and ebola viruses [10, 11]. The ability of suramin to inhibit heparanase expression has been shown to cure the metastasis and proliferation of ovarian, cervical cancer cell lines [12]. In addition the pediatric approved drug has been found to decrease the peak viral load in rhesus monkeys, marking it as a possible therapy for severe EV71 infection in children [13].

In this work we continue to explore the efficacy of suramin against VL, both *in vitro* and in an *in vivo* BALB/c mice model. In addition, its biophysical interaction with the Leishmanial glycolytic enzyme phosphoglycerate kinase (LmPGK) has also been characterized in terms of enzymatic assays and isothermal titration calorimetry (ITC).

Methods

Ethics statements

BALB/c mice (*Mus musculus*) were maintained under pathogen free conditions. The experimental use of mice was approved by the Institutional Animal Ethics Committee of Bose Institute Kolkata, India (dated 26.02.2019; Ref. No. IAEC/BI/121/2019). All animal experiments were carried out according to the National Regulatory Guidelines issued by Committee for the Purpose of Control and Supervision of Experiments on Animals (CPCSEA), Ministry of Environment and Forest, Govt. of India.

Effect of suramin on *Leishmania donovani* (AG83) promastigotes

Measurement of drug efficacy of suramin. *L. donovani*(MHOM/IN/83/AG83) was routinely cultured at 22°C in M199 medium (St. Louis, MO, USA) with 10% heat-inactivated Fetal Bovine Serum(FBS) (Gibco, USA).

L. donovani (AG83) promastigotes were used to determine the efficacy of suramin (IC_{50}) using the MTT assay [8]. Briefly, *L. donovani* parasites were plated on 96-well cell culture plates at a density of 2×10^6 parasites/well and incubated with different concentrations (10 μ M, 20 μ M, 50 μ M, 100 μ M, 300 μ M and 500 μ M) of suramin for 48 hrs. The GraphPad Prism 5 software (version 5.03) was used to calculate the concentration which inhibited parasitic growth by 50% (IC_{50}). Suramin which was used in all the experiments was purchased from Sigma-Aldrich (USA).

Cytotoxicity in RAW 264.7 macrophages. Murine Macrophage (MØs) like tumor cell, RAW 264.7 was obtained from American Type Culture Collection and maintained in complete RPMI 1640 medium supplemented with 10% FBS at 37°C and 5% CO₂ atmosphere. For cytotoxic evaluation, Raw 264.7 macrophages (at a density of 10^5 cells/well) were plated in 96-well cell culture plates and incubated with different concentrations of suramin (1–400 μ M) for 48hrs [14]. Cell viability was determined by the MTT assay and the 50% cytotoxic concentration (CC_{50}) was calculated as stated earlier [8].

Investigation of cell cycle. Cell cycle analysis of suramin for both treated and untreated *L. donovani* promastigotes was investigated using flow cytometry. After treatment of promastigotes (2×10^6 /ml) with varying concentrations of suramin for 48 hrs, the cells were harvested and washed thrice with PBS and fixed in 70% ethanol (24 hrs). The fixed cells were washed thoroughly (three times) with PBS and suspended in 500 μ l of the same buffer. These cells were then incubated with 20 μ g/ml RNase A for 1hr at 37°C and subsequently stained with 20 μ g/ml PI (for 20 minutes at room temperature). The percentage of cells in G1, S and G2/M phases of the cell cycle were determined in the flow cytometer (BDLSRFortessaTMSORP) and analysed with BDFACSDIVA software version 8.0.2

Evaluation of PE-Annexin V/ 7-amino-actinomycin D (7-AAD) binding of cells through flow cytometry. To discriminate between apoptotic or necrotic cell populations, the PE-Annexin V / 7-amino-actinomycin D (7-AAD) apoptosis detection kit (BD Biosciences, USA) was used according to the manufacturer's protocol. Untreated and drug treated (48 hrs) promastigotes (2×10^6 /ml) were washed with cold PBS. The pellets were resuspended in 100 μ l of 1X binding buffer and transferred to a 5 ml culture tube followed by incubation (25 min in the dark) with 5 μ l of PE Annexin V and 5 μ l PerCP-cy5.5-(7-AAD). Finally, the samples were subjected to flow cytometric analysis in a BD LSRFortessaTMSORP flow cytometer, within an

hour of adding 400 μ l of 1X binding buffer to the above solutions. The experimental results were analyzed using the BDFACSDIVA software version 8.0.2 supplied with the instrument.

Measurement of mitochondrial transmembrane potential. Transmembrane potential ($\Delta\Psi_m$) was measured using 5,5',6,6'-tetrachloro-1,1',3,3'-tetraethylbenzimi-dazolylcarbocyanine iodide (JC-1) dye [15]. Briefly, to evaluate the effect of suramin on the mitochondrial membrane potential, *L. donovani* promastigotes (2×10^6 /ml) were incubated with suramin concentrations of 50 μ M, 100 μ M, 200 μ M for 48 hrs at 22°C. Untreated and suramin treated *Leishmania* promastigotes were incubated with JC-1 for 25 min in the dark followed by washing the stained cells twice in PBS. Subsequently, the cell pellets were resuspended in 0.5 ml PBS and subjected to flow cytometry analysis in a BDLSR Fortessa analyzer using an excitation wavelength of 488 nm and emissions at 530 nm (green), 590 nm (red). The results were analyzed by the BDFACSDIVA software version 8.0.2.

Measurement of reactive oxygen species (ROS) generation. Intracellular ROS levels were measured in suramin-treated and untreated parasites. Promastigotes (2×10^6 cells/ml) were treated with suramin and then washed and resuspended in 500 μ l of M199 and incubated with the H₂DCFDA probe (2 μ g/ml) for 20 min in the dark, after which fluorometric measurements (at excitation and emission wavelengths 507, 530 nm respectively) were performed.

Measurement of superoxide radical. Superoxide anion level was monitored as previously discussed [16]. Briefly, 2×10^6 promastigotes/ml were incubated with or without suramin for different time periods and then washed with PBS and resuspended in PBS buffer. Thereafter, the cell suspension was gently mixed with 1mL of reaction mixture containing sodium carbonate (50mM), nitrobluetetrazolium (NBT; 50 μ M), EDTA (0.1mM), Triton X-100 (0.5%) and analysed by spectrophotometer at 560nm wavelength.

Evaluation of total fluorescent lipid peroxidation product. 2×10^6 promastigotes/ml were treated with suramin for different time periods, then washed with PBS and suspended in 2ml of 15% SDS in PBS solution. Subsequently, the cell suspension was used to measure the fluorescence intensities of the total fluorescent lipid peroxidation product [17] on a spectrofluorometer (with excitation and emission at 360nm,430nm respectively).

DNA fragmentation assay. Parasitic genomic DNA was isolated as described previously [18] to perform the genomic DNA fragmentation assay. Briefly, promastigotes (2×10^6 cells) were incubated with varying concentrations of suramin and then harvested. The cell pellet was suspended in 400 μ l NET buffer and incubated for two hrs at 37°C in presence of 100 μ g/ml proteinase K and 1% SDS, following which the DNA was prepared from the samples by phenol chloroform extraction and ethanol precipitation. Finally 1.5% agarose gel electrophoresis was performed to assess the integrity of the parasitic genome.

Effect of suramin on an *in vivo* BALB/c mice model

Infection of mice and suramin treatment regimen. 4–6 weeks BALB/c mice (*Mus musculus*) of the same sex (20–25g) were challenged with freshly transformed AG83 parasites (1×10^7 parasites/animal) by intravenous injection via the tail vein [19]. Suramin treatment commenced 15 days post infection at a dose of 20 mg/kg/day [20] administered intraperitoneally twice a week. The treatment continued for another 15 days and the mice were sacrificed on the seventh day after the termination of the treatment. The BALB/c mice had been grouped into:

- I. normal group: 5 healthy control animals without either infection or drug treatment (Normal)
- II. infected group: 10 animals infected with AG83(INF)

- III. infected+treated group: from the 10 infected animals in (II-INF), 5 animals were treated with suramin (INF+TRE) and
- IV. only treated group: 5 animals were treated with suramin without prior infection to estimate the toxicity of the drug (ONLY TRE).

Blood collection and preparation of serum. Blood was collected from the BALB/c mice heart before sectioning [21] and kept overnight at 4°C. The serum was prepared from the collected blood samples by appropriate centrifugation.

Parasite burden in spleen and liver. Visceral infection was estimated by the microscopic evaluation of Giemsa stained tissue imprints from the spleen and liver and the total parasite load in each organ reported in LDU units (Leishman-Donovan Unit) [22]. LDU = number of amastigotes per nucleated cell x organ weight in milligram.

Preparation of soluble Leishmanial antigen (SLA). Preparation of Leishmanial lysates from stationary phase promastigotes (10^9 cells/ml) has been reported previously [23]. *Leishmania* promastigotes were partially lysed by six cycles of freezing (-70°C)—thawing (37°C), after which the sample was incubated for five minutes on ice. This was followed by sonication (5 times—30s), centrifugation (10000 rpm for 30 min at 4°C) and the protein concentration inclusive of the soluble antigen in the supernatant, was measured using the Bradford reagent (BioRAD).

T-cell proliferation assay. Splenocytes from the BALB/c mice were extracted by Ficoll density gradient centrifugation and then suspended in RPMI medium followed by plating on 96 well plates (10^5 cells/well), which were then allowed to proliferate for 72 hours (at 37°C) in a 5% CO₂ incubator, appropriately in the presence or absence of SLA (5 µg/ml) or ConA (5 µg/ml). Finally, these cells were subjected to MTT assay (absorbance at 570 nm). Effect of suramin on splenic CD4⁺ and CD8⁺ T cell populations was also investigated. Single cell suspension (2×10^6 per tube) of splenocytes was washed twice with FACS buffer (1% BSA in PBS) and stained with antimouse-CD4-FITC (Santacruze Biotech) and antimouse-CD8a PercP antibodies (BD Pharmingen™) at 1:500 dilution for 60 min in the dark at 4°C. The cells were then subjected to flow cytometry analysis in a BDLSR Fortessa analyzer and respective percentages of CD4⁺ and CD8⁺ cells were determined using BD FACSDIVA software.

Measurement of antileishmanial antibody responses. Serum samples collected from mice were used to investigate the parasite SLA-specific antibody titer. IgG1 and IgG2a present in the collected sera were estimated with the HRP conjugated Goat Anti-Mouse IgG1 and IgG2a antibodies (Abcam: ab97240; ab97245) as described elsewhere [24].

Measurement of Nitric oxide (NO) and Reactive Oxygen Species (ROS). Splenocytes (2×10^6 cells/well) were incubated with 5 µg/ml SLA in a 5% CO₂ incubator (at 37°C for 48 hrs) followed by the collection of the culture supernatants. The NO production in the culture supernatant was measured by the Griess reagent [25]. To measure the ROS level, splenocytes were stimulated with respective SLA for 24 hrs. The splenocytes were then washed and resuspended in PBS followed by incubation with the probe H₂DCFDA (2 µg/ml) at room temperature for 20 min in the dark [25]. Fluorimetric measurements were made on the samples with excitation, emission wavelengths of 510, 525 nm respectively and the results were expressed in arbitrary units.

RNA isolation and semi quantitative RT-PCR of iNOS, Perforin and Granzyme-B. To detect the mRNA profiles of iNOS, perforin and granzyme-B, total RNA was isolated from the splenocytes of different mice groups as described earlier [6]. RNA (2.5 µg) was used as a template for cDNA synthesis and the respective forward and reverse primers (S1 Table) were used for determination of iNOS, perforin and granzyme-B expressions respectively. PCR cycling

conditions for the amplification of specific genes were 5 min at 94°C, followed by 35 cycles of denaturation at 94°C for 30s, annealing at (58°–60°C) for 30s and extension at 72°C for 45s. All the tubes were kept for 5 min at 72°C for extension to go to completion. PCR-amplified respective gene products were checked by agarose gel electrophoresis. For densitometry analyses, the Image J software (National Institute of Health) was used and the same band area in the agarose gel was used to determine band intensity and normalized for GAPDH.

Measurement of cytokine levels. The T_H1 (IFN- γ , IL-12 and TNF- α) and T_H2 (IL-10, TGF- β) cytokine productions were measured by the ELISAmethod [26]. 2x10⁶ splenocytes were plated on 24-well tissue culture plates and pulsed with 5 μ g/ml SLA, after which the supernatant was collected within 18–20 hrs and ELISA performed on the collected supernatants as per the manufacturer's instructions (Abcam: TNF- α , TGF- β ; BD Biosciences: IFN- γ , IL-12, IL-10).

Characterization of Protein–drug interaction

Protein expression, purification. The plasmid constructs containing Phosphoglycerate kinase (LmPGK) [Accession code XP_001682765.1] were purchased from GenScript (<http://www.genscript.com>).

The plasmid construct was prepared by inserting the gene (LmPGK) between the Nde1 and BamH1 restriction sites of the pET-28a (+) vector. This construct was used to transform *E. coli* BL21 competent cells followed by overnight incubation on LB-agar/kanamycin plates at 37°C. A single colony was isolated from each plate and used to inoculate LB media containing kanamycin. Induction by IPTG (final concentration 0.75mM) was performed when OD600 attained a value of ~0.6, followed by overnight incubation at 20°C. The cells were harvested by centrifugation at 7500rpm for 10 minutes and washed with PBS buffer. The cell pellets were then suspended in lysis buffer (50mM NaH₂PO₄, pH 8.0, 300mM NaCl, 10mM imidazole, 5% glycerol) and the cell suspension sonicated, centrifuged at 14500rpm for 30 minutes at 4°C and the supernatant collected. Pre-equilibrated Ni-NTA column (QIAGEN Ni-NTA super flow) was used to purify the supernatants. The column was washed with 100 ml of wash buffer (50mM NaH₂PO₄, pH 8.0, 300mM NaCl, 50mM imidazole, 1% glycerol) and the bound proteins eluted with elution buffer (50mM NaH₂PO₄, pH 8.0, 300mM NaCl, 250mM imidazole, 1% glycerol). The eluted LmPGK protein was dialyzed overnight against the storage buffer (80mM triethanolamine HCl, pH 7.6, 200mM NaCl, 3mM DL-dithiothreitol, 1% glycerol, 0.02% sodium azide). The N-terminal 6-His tag was excised by thrombin cleavage which was subsequently removed from the protein solution by streptavidin agarose (as per the manufacturer's instructions: Novagen).

Isothermal Titration Calorimetry (ITC). Isothermal titration calorimetry (ITC) was performed using an ITC 200 Micro calorimeter at 25°C to determine the binding of suramin with LmPGK in 25mM Tris-HCl buffer, pH 7.0. Typically, 2 ml of LmPGK (15 μ M) was loaded into the calorimetric cell and titrated against 320 μ M of suramin (single injection of 2 μ l followed by injections of 10 μ l each) using a 39.4 μ l syringe rotating at 307 rpm, with a reference power of 8 μ cal/sec. Controls involved identical titrations of buffer alone to optimize the data for heat of dilutions. Corrected thermograms were analyzed for a single site binding model using Levenberg-Marquardt non-linear least squares curve fitting algorithm, Origin 7.0 software (Origin Lab Corporation, USA: supplied with the instrument) to obtain best fit values.

3c. Enzyme inhibition assay. The *in vitro* assay of LmPGK was monitored by UV–vis spectroscopy in a coupled assay wherein, the product of the first reaction catalyzed by LmPGK, namely 1, 3- bisphosphoglycerate is reduced by the second enzyme glyceraldehyde-3-phosphate dehydrogenase, utilising NADH. The enzymatic assays were performed in

80mMtriethanolamine-HClbuffer (pH-7.6) containing 5mM MgSO₄, 1mM ATP, 0.5mM NADH, 30μg/ml of glyceraldehyde-phosphate dehydrogenase and approximately 10nM of LmPGK, for each assay [27]. The concentration of the substrate (3-phosphoglycerate) was maintained between 250μM to 5mM whereas the inhibitor (suramin) concentration was varied from 5μM to 15μM. The spectrophotometric measurements were carried out at 25°C, following the decrease in absorbance at 340 nm due to oxidation of NADH and formation of NAD⁺ at $\lambda = 340$ nm ($\epsilon_{340\text{nm}} = 6.3 \text{ mM}^{-1} \text{ cm}^{-1}$) [28]. Kinetic parameters were determined by using Michaelis–Menten kinetics and the inhibition constants were determined from the initial velocity data. The Lineweaver–Burkeplots [29] were obtained from the following general equation:

$$\frac{1}{v} = \frac{K_M}{V_{\max}} \left(1 + \frac{[I]}{K_i} \right) \frac{1}{[S]} + \frac{1}{V_{\max}} \left(1 + \frac{[I]}{K_i} \right)$$

where v is the initial velocity, $[S]$ is the substrate concentration, $[I]$ is the inhibitor concentration, K_M the Michaelis constant and K_i the inhibitor constant, V_{\max} is maximum velocity.

Results

Effect of Suramin on *L. donovani*(AG83) promastigotes

The IC₅₀ value of suramin against *L. donovani*(AG83) promastigotes was determined to be 100.0±4μM. The CC₅₀ against RAW 264.7 macrophages was 51±5μM and the corresponding EC₅₀ value of suramin against intracellular *L. donovani*(AG83) amastigotes had earlier been reported to be 4.1±0.3 μM [8].

Leishmania promastigotes were exposed to varying concentrations of suramin and the distribution of promastigotes (%) in different phases of the cell cycle was analyzed by flow cytometry. Only 8.4±0.9% of untreated control cells were found in the G2/M phase. In contrast, increasing concentrations of suramin (50, 100, 200 μM) led to a progressively increasing accumulation of cells in the G2/M phase (11.5±1.7, 19.6±2.9 and 24.2±1.4% respectively), thereby indicating arrest of the promastigote cell cycle at G2/M upon exposure to the drug (Fig 1).

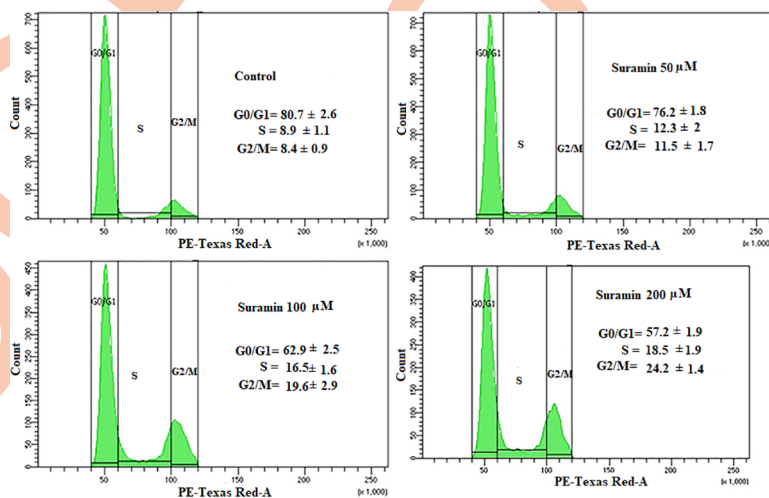


Fig 1. Analysis of cell cycle arrest in *L. donovani* promastigote treated with suramin. The histograms are representative of three independent experiments. AG83 promastigotes with (50, 100, 200 μM suramin) or without the drug were analyzed by flow cytometry on a BD LSRFortessa™ SORP cytometer. The histograms depict the accumulation of the cells in different phases of the cell cycle as a function of suramin concentration. Percentage of cells in different phases has been given within the histogram boxes and the results show the dose dependent accumulation of cells in the G2/M phase.

<https://doi.org/10.1371/journal.pntd.0008575.g001>

In order to further discriminate the mode of cell death, AG83 promastigotes were double stained with PE-Annexin V, 7-AAD and then followed by flow cytometric measurements. For untreated control cells only 1.1% of the promastigotes were found in the early apoptotic phase [annexinV(+), 7-AAD(-)]. However, upon suramin treatment a dose dependent increase in the percentage of cells at early apoptotic phase was observed-18.4% (suramin 50 μ M), 37.5% (suramin 100 μ M) and 58% (suramin 200 μ M), with respect to the untreated control (Fig 2).

As apoptosis is generally associated with disruption of normal mitochondrial function, perturbations in mitochondrial membrane potential $\Delta\psi_m$ was estimated in AG83 promastigotes. Administration of suramin was found to exhibit a dose-dependent increase in green fluorescence indicative of a loss in membrane potential and a corresponding decline in the red/green fluorescence intensity ratio, after 48 hours of incubation with the drug (Fig 3). For untreated control, the percentage of cells in the red and green regions was 82.2 and 17.6% respectively. With a graduated increase in the drug dosage, the distribution of treated cells in the red and green regions (respectively) were altered to 75.3, 24.4% (50 μ Msuramin), 68.3, 31.1% (100 μ Msuramin) and 48.4, 42.9% (200 μ M), thereby confirming the involvement of the apoptotic pathway in cell mortality.

Three other experiments indicated the disruptive effect of suramin in the viability of the parasite. Increasing concentrations of suramin led to a higher generation of reactive oxygen species (Fig 4A), rising levels of intracellular superoxide radicals (Fig 4B) and increased lipid peroxidation (Fig 4C) relative to untreated controls. All the three experiments affirmed elevated oxidative stress in the parasite inimical to its survival. Further, the addition of suramin appeared to cause fragmentation of the genomic DNA (Fig 5), the hallmark of apoptosis.

Efficacy of Suramin in a *Leishmania* infected BALB/c mice Model

The VL mice model was established with freshly transformed *L.donovanipromastigotes* following which the infected animals were treated with suramin (20 mg/kg/day, twice a week for 15 days) and then sacrificed for investigation on the seventh day after the termination of the treatment. At a dose of 20 mg/kg/day there was a reduction in the hepatic parasitic load by 84.3 \pm 8.2% (Fig 6A) and a corresponding drop in the splenic parasitic load by 87.4 \pm 5.2% (Fig 6B).

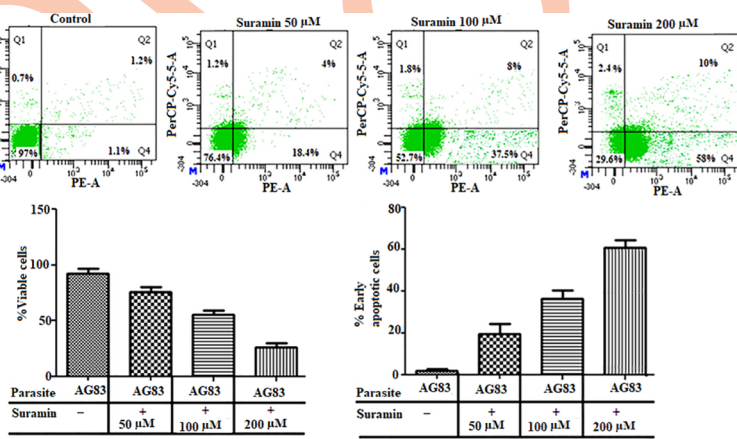


Fig 2. Flow cytometric analysis of viable cell populations after suramin treatment. Dotplots are representative of three independent experiments. AG83 promastigotes were double stained with PE-Annexin V and 7-AAD and then subjected to flow cytometry analyses on a BD LSRFortessa™ SORPflow cytometer. The experiments were repeated with untreated cells and those subject to varying doses of suramin (50, 100, 200 μ M). In the plots the green dots in the fourth quadrant (Q4) depict cells in the early apoptotic phase. The bar diagrams give the percentage of viable and early apoptotic cells, in the presence and absence of the drug (concentration given in boxes below). A dose dependent increase of cells in the early apoptotic phase was observed under varying concentration of the drug.

<https://doi.org/10.1371/journal.pntd.0008575.g002>

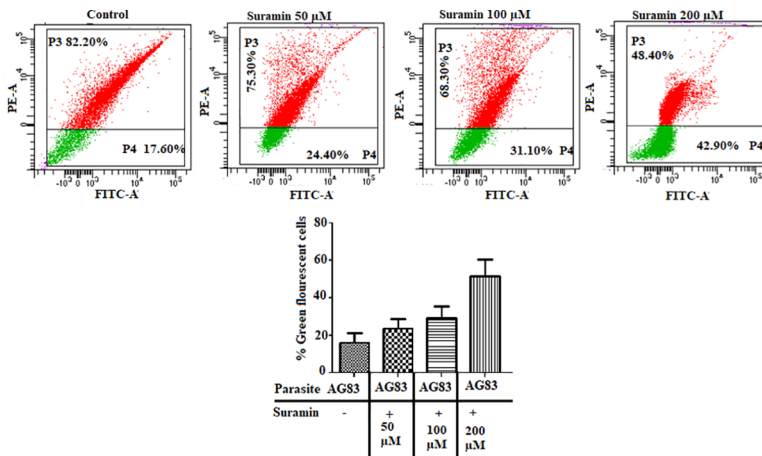


Fig 3. Effect of suramin on mitochondrial membrane potential ($\Delta\psi_m$). *L. donovani* promastigotes (AG83), untreated and treated with varying concentrations of suramin (50,100,200 μ M) and stained with JC-1 were analyzed with flow cytometry on a BDLSR Fortessa analyzer with excitation wavelength at 488 nm and emission wavelengths 530 (green), 590 nm (red). The dot plots are representative of three independent experiments. The bar diagrams plot the percentage of green fluorescent cells as a function of suramin concentration given in the boxes below. The results show a dose dependent increase in green fluorescent cells with a loss in membrane potential thereby indicating the apoptotic pathway as the cause of drug induced cell mortality.

<https://doi.org/10.1371/journal.pntd.0008575.g003>

Next, the role of suramin in the generation of effector leishmanicidal molecules such as ROS and NO were estimated. Suramin-treated mice (INF+TRE) showed 4.05 fold higher ROS generation compared to the corresponding infected group (INF) (Fig 7A). NO generation was

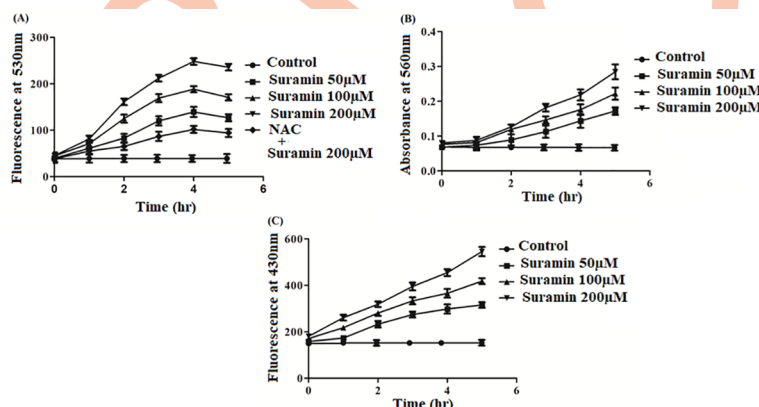


Fig 4. Estimation of (A)ROS, (B)superoxides and(C)lipid peroxidation levels in promastigotes after suramin treatment. All experiments were performed with 2×10^6 promastigotes/ml and the depicted data is the mean \pm SD of three experiments. (A) Intracellular ROS production with and without suramin was estimated in promastigotes utilizing the probe H₂DCFDA coupled to fluorometric measurements (excitation, emission wavelengths at 507, 530 nm respectively). The figure shows elevated ROS production with rising concentrations of suramin (50,100,200 μ M) treatment. The inhibition of ROS generation was shown at the highest concentration of suramin (200 μ M) by pretreatment of cells with 20mM N-acetylcysteine (NAC: a scavenger of ROS). (B) Superoxide generation in AG83 promastigotes was estimated by measuring the absorbance at 560 nm subsequent to appropriate treatment of the cells. Superoxide generation was measured at suramin concentrations 50, 100, 200 μ M, in addition to untreated controls. The figure demonstrates the rise in superoxide levels with increasing drug concentrations. (C) Fluorescent products of lipid peroxidation measured by a spectrofluorimeter with excitation and emission wavelengths at 360, 430 nm respectively, with and without suramin treatment (50, 100, 200 μ M). The graduated rise in all the three parameters ROS, superoxide radicals and lipid peroxidation is indicative of elevated oxidative stress in the parasite upon suramin administration, inimical to survival.

<https://doi.org/10.1371/journal.pntd.0008575.g004>

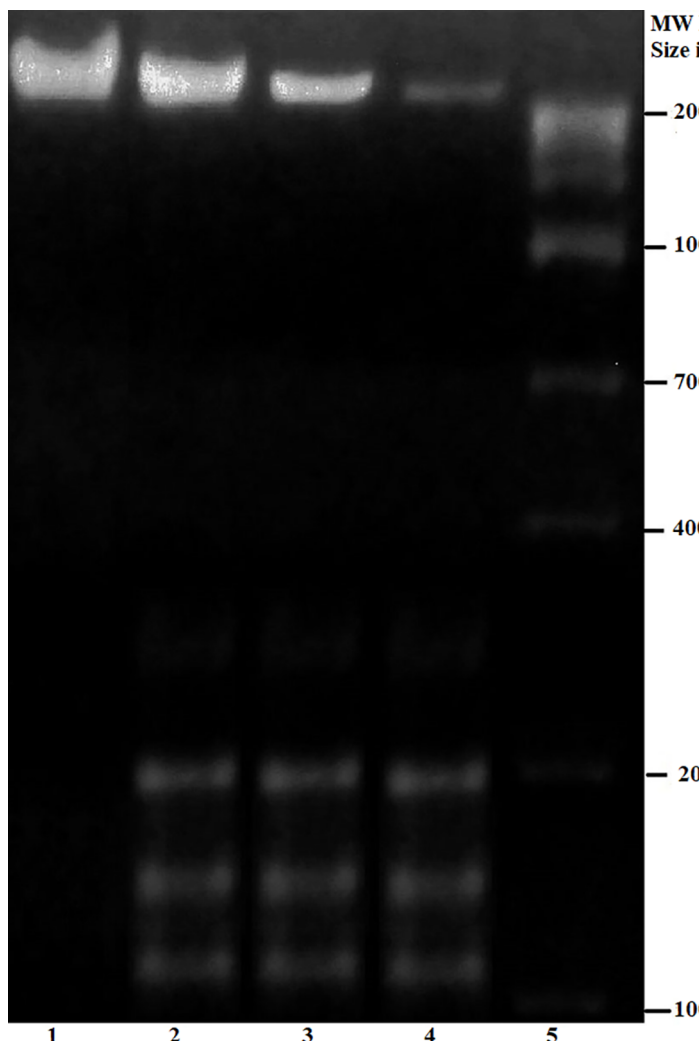


Fig 5. Fragmentation of genomic DNA in the presence of suramin compared to untreated control. Parasitic DNA was isolated from promastigotes subjected to varying concentrations of suramin and the integrity of the genome assessed by running the extracted DNA on a 1.5% agarose gel. The lane number is marked below. **Lane 1:** Untreated control without suramin treatment; **Lane 2:** Genomic DNA was isolated from AG83 promastigotes treated with 50 μ M suramin; **Lane 3:** Genomic DNA was isolated from AG83 promastigotes treated with 100 μ M suramin; **Lane 4:** Genomic DNA was isolated from AG83 promastigotes treated with 200 μ M suramin; **Lane 5:** Molecular weight marker.

<https://doi.org/10.1371/journal.pntd.0008575.g005>

measured in the culture supernatant of murine splenocytes isolated from all the experimental groups. Suramin-treated mice (INF+TRE) showed a significantly higher level of NO generation compared to the corresponding infected group (INF) (Fig 7B). Consistent with NO generation, the levels of iNOS mRNA were also upregulated post suramin treatment in the INF+TRE group (S1 Fig, Fig 7C). Thus, these series of experiments indicated that subsequent to the administration of the drug, the infected animals recovered from their state of immune suppression and could induce leishmanicidal molecules to significantly reduce the parasitic burden in the hosts.

Reduction of parasitic burden and induction of antileishmanial molecules, prompted us to examine whether suramin is associated with an effective immune response against VL. To this end, the expansion of the antigen-specific T-cell repertoire was measured in all the experimental groups. Suramin-treated mice (INF+TRE) exhibited enhanced level of T cell proliferation

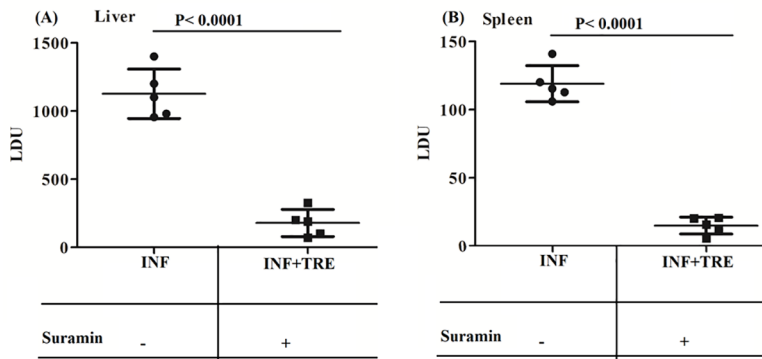


Fig 6. Estimation of parasite burden in the spleen and liver of the experimental group of animals: (A) Liver and (B) Spleen. Total parasite load in liver and spleen was estimated by the microscopic evaluation of Giemsa stained tissue from the corresponding organs and is expressed in LDU (Leishman-Donovan) units; where LDU = number of amastigote per nucleated cell x organ weight in milligram. The results are the mean±SD of 5 animals per group and unpaired two-tailed Student's t-test was performed to determine the levels of significance indicated by P values. Treatment with (+) and without (-) suramin is indicated in the box below. At a dose of 20mg/kg/day (twice a week for 15 days) there are significant reductions in the hepatic (A) and splenic (B) parasitic loads respectively.

<https://doi.org/10.1371/journal.pntd.0008575.g006>

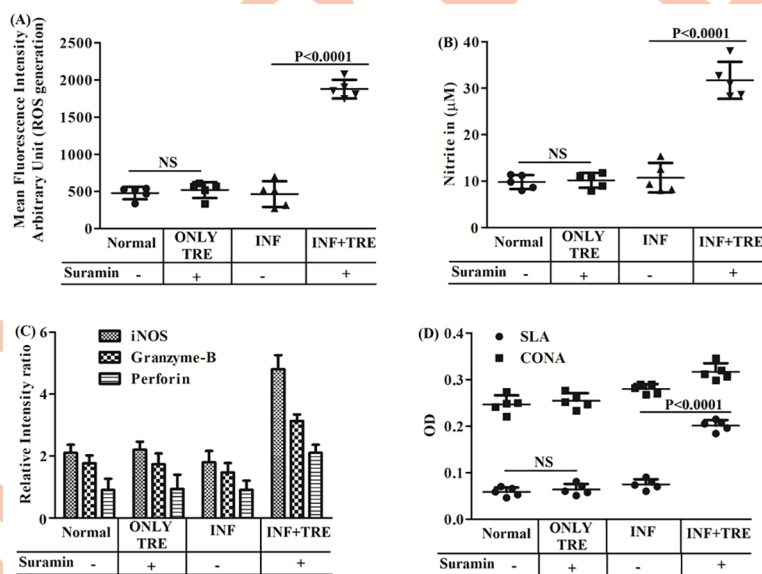


Fig 7. In vivo generation of (A) ROS and (B) NO (C) Semiquantitative RT-PCR of iNOS, Granzyme-B, Perforin and (D) T-cell proliferation assay for all the experimental group of BALB/c mice. Results are averaged (mean±SD) over 5 animals per group (Normal, ONLY TRE, INF and INF+TRE in the boxes below) and unpaired two-tailed Student's t-test performed to indicate levels of significance by P values with statistical insignificance denoted by NS. (A) ROS and (B) NO production were estimated with the probe H₂DCFDA and the Griess reagent respectively and both are upregulated in INF+TRE relative to other groups. (C) mRNA expression levels of iNOS, Granzyme-B and Perforin from the splenocytes from the different mice groups were measured by semi quantitative RT PCR utilising specific primers and expressed as a ratio to GAPDH mRNA levels. Densitometric data are plotted for graphical reorientations and all the three genes exhibit significantly elevated expression levels in the suramin treated INF+TRE group. (D) T cell proliferation was estimated after stimulation of splenocytes either with SLA (5 $\mu\text{g}/\text{ml}$) or with non-specific mitogen ConA (5 $\mu\text{g}/\text{ml}$) followed by an MTT assay and the data suggests that the splenocytes of suramin treated (INF+TRE) stimulated with SLA promotes the expansion of antileishmanial T cell repertoire relative to controls.

<https://doi.org/10.1371/journal.pntd.0008575.g007>

compared to infected (INF) group (Fig 7D). To further confirm that the suraminmediated proliferative response of splenocytes is primarily contributed by T cells, splenic CD4⁺ and CD8⁺T cell populations were estimated. The expression levels of both CD4⁺ and CD8⁺T cells were upregulated in the INF+TRE group compared to the corresponding INF group (S2 Fig). Expression levels of granzyme-B and perforin were also enhanced in the INF+TRE group (S1 Fig, Fig 7C). Hence, suramin could possibly activate the CD4⁺T-cells while elevated expression levels of perforin and granzyme-B appear to indicate the supportive protection of the host via CD8⁺T cells, in the INF+TRE group of animals.

Next, T_H1 (IFN- γ , TNF- α , IL-12) and T_H2 (IL-10, TGF- β) cytokine responses were investigated by ELISA to evaluate the immunological response associated with suramin treatment. The enhanced level of T_H1 cytokine in suramin-treated mice was manifest with higher IFN- γ secretion (approximately 3.3 fold) in (INF+TRE), relative to (INF) (Fig 8A). The increased level of IFN- γ production was also in correspondence with the upregulation of other pro-inflammatory cytokines such as of TNF- α and IL-12. TNF- α and IL-12 responses in the INF+TRE group were enhanced 4.2, 5.0 times respectively compared to the corresponding INF (Fig 8B and 8C).

T_H2 cytokines play a vital role in disease progression and immune suppression. Inhibition in the production of some these cytokines indicates recovery from the disease [30]. Suramin-treated animals (INF+TRE) exhibited about 3.1 fold decrease in IL-10 production (Fig 8D) while a 3.5 fold drop in TGF- β levels was observed in the same group (Fig 8E), compared to INF.

Earlier reports have confirmed that disease progression in leishmaniasis is associated with altered levels of specific antileishmanial antibodies [31]. Immunoglobulins such as IgG1 and IgG2a production can be used as surrogate markers for T_H2 and T_H1 cytokine responses respectively and significant increase in IgG2a levels is generally held to be indicative of successful immune response [32]. Estimation of IgG2a and IgG1 levels in the sera of all the animal groups (Fig 9), exhibited a reduction in the level of IgG1 isotype for the INF+TRE group

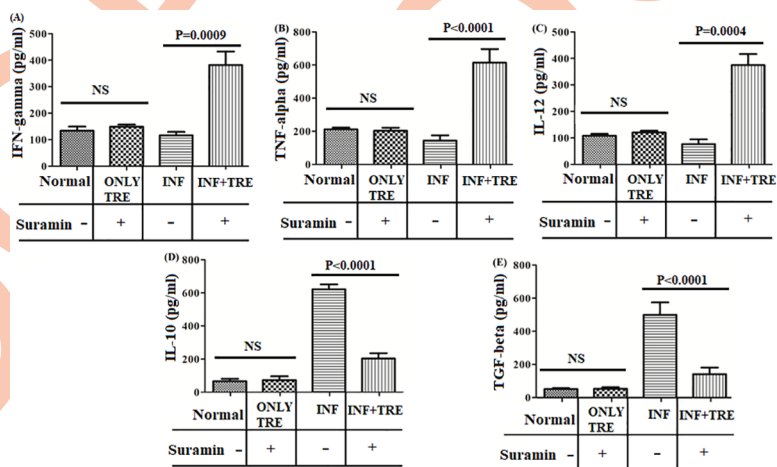


Fig 8. Assessment of T_H1 and T_H2 cytokine productions in all the experimental group of animals (Normal, ONLY TRE, INF, INF+TRE). T_H1 and T_H2 cytokine generation assayed by ELISA performed on the supernatants collected from mice splenocytes pulsed with SLA, from the different groups (given in the boxes below the bar diagrams) for (A) IFN-gamma (B) TNF-alpha, (C) IL-12, (D) IL-10, (E) TGF-beta cytokine levels. Unpaired two-tailed Student's t-test was performed and levels of significance indicated by P values with NS denoting statistical insignificance. The results show a significant increase of pro-inflammatory T_H1 cytokines in INF+TRE relative to INF, with a decrease in T_H2 cytokines indicative of recovery from infection.

<https://doi.org/10.1371/journal.pntd.0008575.g008>

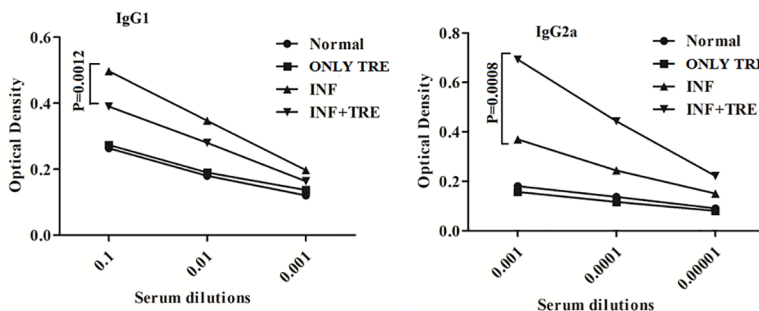


Fig 9. Measurement of antileishmanial IgG1 and IgG2a antibody titers in different group of animals. Serum samples from mice were used to estimate the levels of IgG1 and IgG2a respectively. The dilutions of sera 10^{-1} , 10^{-2} , 10^{-3} fold were used to analyze IgG1 and 10^{-3} , 10^{-4} , 10^{-5} fold were used to analyze IgG2a levels in all experimental groups (Normal, ONLY TRE, INF, INF+TRE). Unpaired two-tailed Student's t-test was performed and levels of significance indicated by P values with NS denoting insignificance. The experiment demonstrated an increase in the IgG2a levels in INF+TRE with respect to other groups, generally indicative of successful immune response.

<https://doi.org/10.1371/journal.pntd.0008575.g009>

[$P = 0.0012$ at 10^{-1} dilution)] while an increase in the IgG2a levels was observed for the same group ($P = 0.0008$ at 10^{-3} dilution) with respect to INF (Fig 9).

Characterization of protein-drug interaction

PGK-suramin interaction has been confirmed by ITC (Fig 10A). The figure shows a representative titration curve that fits well to a 'single binding site' model. A detailed listing of all thermodynamic parameters is given in Table 1. The dissociation constant (K_d) for the reaction between PGK and suramin was estimated to be of $4.27\mu\text{M}$ at 25°C , with favourable enthalpic ($\Delta H: -6.11 \pm 0.26 \text{ kcal mol}^{-1}$) and entropic ($T\Delta S: 0.277 \text{ kcal mol}^{-1}$) contributions. Survey of

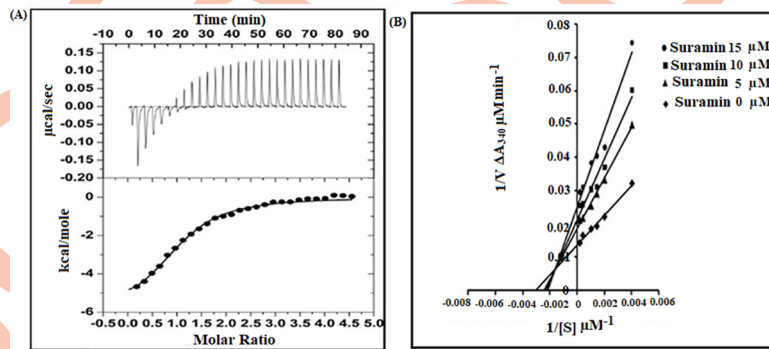


Fig 10. (A) PGK- suramin interaction studied by isothermal titration calorimetry (ITC). Thermogram obtained from an ITC 200 Microcalorimeter at 298 K to estimate the binding of LmPGK and suramin in 25mM Tris-HCl buffer. The corrected thermogram was analyzed using Levenberg-Marquardt non-linear least squares curve fitting algorithm, Origin 7.0 software. The stoichiometry of LmPGK-suramin interaction was 1:1 with a dissociation constant (K_d) of $4.27\mu\text{M}$, sustained by favourable entropic and enthalpic contributions. (B) Lineweaver-Burk plots for inhibition of LmPGK by suramin. A coupled assay at 25°C was used to assay LmPGK(10 nM) by uv-vis spectroscopy wherein the product of LmPGK namely 1, 3-biphosphoglycerate was reduced by glyceraldehyde-3-phosphate dehydrogenase ($30\text{ }\mu\text{g/ml}$) utilising NADH (0.5 mM). The formation of NAD^+ was monitored at 340 nm . The reaction was carried out in triethanolamine-HCl buffer ($\text{pH } 7.6$) with the substrate 3-phosphoglycerate concentration varying from $250\text{ }\mu\text{M}$ - 5 mM and suramin $5\text{--}15\text{ }\mu\text{M}$ (V denoting initial velocity and $[S]$ substrate concentration). The kinetic parameters and inhibition constant was determined from the initial velocity using Michaelis-Menten kinetics. A mixed type of inhibition was observed with the K_m , V_{max} and inhibition constant being $322.87\text{ }\mu\text{M}$, $72.7\text{ }\mu\text{M}/\text{min}$ and $8.7 \pm 1.3\text{ }\mu\text{M}$ respectively. ((●) suramin concentration $15\mu\text{M}$; (■) suramin concentration $10\mu\text{M}$; (▲) suramin concentration $5\mu\text{M}$; (◆) suramin concentration $0\mu\text{M}$).

<https://doi.org/10.1371/journal.pntd.0008575.g010>

Table 1. Thermodynamic parameters for the formation of LmPGK-suramin binary Complex by isothermal titration calorimetry (ITC).

System	Temp (K)	[drug/protein] N	$K_a \cdot 10^5$ (M ⁻¹)	ΔH kcalmol ⁻¹	$T\Delta S$ kcalmol ⁻¹	ΔG kcalmol ⁻¹
Thermo dynamic data	298	1.07±0.0346	2.34±0.25	-6.11±0.26	0.277	-6.387

<https://doi.org/10.1371/journal.pntd.0008575.t001>

suramin–protein (pyruvate kinase) interactions in a complex crystal structure (PDB Code:3PP7) [33] reveals extensive hydrophobic stacking interactions of the naphthalene ring coupled with hydrogen bonds involving the sulphur bound and carbonyl oxygens of the drug. The entropic contribution could possibly arise due to the displacement of water molecules from the binding site of the protein upon association with suramin.

The above observation was also substantiated by enzyme inhibition study which confirmed the enzymatic inhibition of LmPGK by suramin (Fig 10B). The kinetic parameters Km, Vmax for the enzymatic function of LmPGK with respect to its substrate 3- phosphoglycerate was determined to be 322.87μM and 72.7μM/min respectively. A mixedtype of inhibition was observed for suramin and the inhibition constant was determined to be 8.7±1.3μM as evaluated from the Lineweaver–Burke plot. Thus, a good correlation was observed between the ITC and enzymatic assay data with respect to thermodynamic parameters involving inhibition and dissociation constants.

Discussion

Due to excessive costs involved in drug development, one strategy to identify novel therapeutics would be to re-purpose clinically approved drugs as potential antileishmanials. Of the four drugs (pentamidine, suramin, melarsoprol, and eflornithine) which currently constitute the repertoire to combat human African trypanosomiasis (HAT) [34], pentamidine has earlier been used as a second line drug in the treatment of VL. In this work the efficacy of suramin as a possible antileishmanial compound has been confirmed by *in vitro* and *in vivo* studies, specifically in BALB/c mice. The Leishmanial infection pattern is based on the fact that the parasite has a dimorphological life cycle i.e. promastigote (the infective stage) and amastigote (the intracellular stage). Upon attacking the host macrophage in the mammalian system, promastigotes are internalised (into the macrophage) by phagocytosis and transform to amastigotes by invading the host protective immune response. The parasite then multiplies within the host macrophage and emerges from the host cell by the disruption of its cell membrane. The infection cycle is then repeated on nearby cells by breaching their effective immune barriers where the heightened T_H2 immune response facilitates the immune evasion of the parasite. An effective drug should ideally act simultaneously on both the intracellular and the extracellular forms of the parasite. Our study reveals that suramin effectively induces cellular events characteristic of apoptosis in the *Leishmania* parasite and successfully reduces the intracellular parasitic burden *in vivo* by upregulating the host compromised T_H1 immune response.

Experiments with AG83 promastigotes appear to indicate that apoptosis could be the mode of cell death upon suramin treatment. The cellular symptoms generally associated with apoptosis, which appear on suramin exposure include DNA fragmentation, loss of mitochondrial membrane potential $\Delta\psi_m$ and the increase of early apoptotic cells as a function of drug dosage. Since suramin has been known to target parasitic enzymes involved in glycolysis, the present study serves as another example, where inhibition of glycolytic ATP production coupled to mitochondrial membrane depolarization could possibly lead to apoptotic cell mortality. In cancer cells[35], a preferred mode of treatment involves glycolytic inhibition and consequent

apoptosis by depriving the cells of ATP. Generally, for such cells mitochondrial respiratory dysfunction leads to the rapid dephosphorylation of the (anti apoptotic and glycolysis-apoptosis integrating) BAD protein, relocalization of the BAX molecule to the mitochondria and almost inevitable cell death[35]. In *Leishmania* much remains to be known with regard to the biochemical linkage between glycolysis and apoptosis. However, all three anti-leishmanials-luteolin [36], KalsomeTM10 (a liposomal formulation of amphotericin B)[37] and tafenoquine [38], drastically reduce the intracellular pool of ATP and perturb mitochondrial integrity leading to increased ROS production, stimulation of caspase-like activity, cell cycle arrest, DNA fragmentation and apoptosis. The most fundamental or at least universal event in every case is the rapid drop in cellular ATP levels which could be achieved by alternative methods apart from inhibiting the glycolytic pathway alone, such as in tafenoquine[38], where the disruption of Leishmanial bioenergetics is by the inhibition of cytochrome c reductase (respiratory complex III).

The current experiments involving BALB/c mice indicate that suramin plays a prominent role in stimulating immune response against parasitic invasion. CD4⁺ T_H cells mediate immune response primarily through secreted cytokines and two subpopulations T_H1 and T_H2 of T helper cells can be distinguished based on their repertoire of these molecules[39]. In mice, effective response to Leishmanial infection depends on the preferential activation of the T_H1 cells (relative to T_H2) and the corresponding high levels of associated cytokine IFN- γ [40,41]. In addition cytokine IL-12 has been identified as necessary for the expansion of CD4⁺ T_H1 cells [42]. BALB/c mice display a high propensity of succumbing to the parasite as from an early stage of infection there is a tendency of the immune response to be skewed in favour of T_H2[43]. Direct correlation has also been observed between the T_H2 cytokine IL-10 and progression of VL pathogenesis [30]. The administration of suramin however, appears to consolidate T_H1 activation, evident from a 3.3 fold increase in levels of IFN- γ (in INF+TRE relative to INF) along with other T_H1 cytokines TNF- α (4.2 fold) and IL-12 (5.0 fold). As simultaneous reduction in the levels of T_H2 cytokines IL-10 (3.1 fold) and TGF- β (3.5 fold), were also observed. In addition increase of IgG2a levels in the sera confirmed the decisive tilt in favour of T_H1 type immune response. A similar pattern was also observed for C57BL/6 mice infected with a virulent strain of *Trypanosoma cruzi*, where suramin stimulated the immune system increasing levels of IFN- γ , TNF- α and IgG2a [44]. Thus, the current study appears to confirm that suramin facilitates switching the immunosuppressive humoral response to a host protective T_H1 type associated with the strong generation of effector Leishmanicidal molecules.

In addition to the aggressive activity of CD4⁺ T_H cells, CD8⁺ cytotoxic T lymphocytes (CTLs) could also play either a supporting or synergistic role in the neutralization of *Leishmania* parasites, as both cell populations were found to be upregulated (in INF+TRE) along with elevated expression levels of perforin and granzyme-B. As is well known upon exocytosis from CTLs, perforin mediates granzyme-B entry into the parasitic cell (by pore formation in its cell membrane) and once inside, granzyme-B initiates a cascade of reactions finally resulting in the DNA fragmentation of the target cell[45].

There is a mass of evidence in the literature which demonstrates that suramin is highly promiscuous in its choice of targets thereby exhibiting a broad spectrum of clinical effects[46,47]. It has been shown to inhibit with varying degrees all the seven glycolytic enzymes in *T. brucei* localized in the glycosomes[48] and its crystal structure complexed with pyruvate kinase (from *T. cruzi*) revealed the association of a single drug molecule at the ATP/ADP binding site of the enzyme (by virtue of its poly sulphonate groups)[33]. In addition suramin has been known to inhibit phosphogluconate dehydrogenase of the pentose phosphate pathway [34]. Suramin inhibits both the glycosomal ($K_i^{app} = 8.0 \mu M$) and cytoplasmic ($K_i^{app} = 20.0 \mu M$) isoforms of phosphoglycerate kinase (PGK) in *T. brucei*, competitively with respect to the substrate (3

phosphoglycerate), two drug molecules binding to each protein [9]. In this work drug binding inhibition of cytosolic phosphoglycerate kinase from *L. major* (Accession code XP_001682765.1) has been estimated, which has a sequence identity of 97.1 and 72.1% with respect to the homologous proteins from *L. donovani* (Accession code TPP45561.1) and *T. brucei* (AAA32120.1) respectively. However, in this case the ITC data confirmed a 1:1 stoichiometry between the protein and the drug with a mixed type inhibition ($K_i = 8.7 \mu\text{M}$), indicating that suramin can bind to the LmPGK irrespective of the (bound) presence or absence of the substrate (3 phosphoglycerate), though with different affinities for both states [29].

One disadvantage in the field application of suramin lies in the fact that the effective administration of the drug is only by intravenous injections at a dose of 20mg/kg (spread over a month), as the drug is poorly absorbed in the intestines and intramuscular administration leads to irritation at the site of injection [49]. The exclusive use of intravenous injections for suramin might create logistic problems for drug administration at remote locations. Excessive build up of suramin concentration in the blood stream also leads to toxic side effects (such as fatigue, neuropathy, anaemia etc.) as the long half-life of the drug (about 50 days) ensures that it is retained in the body for weeks at a time [34]. However, the toxicity profile of suramin is by and large completely understood given its long usage in the field for HAT, and its intraperitoneal mouse acute toxicity (LD_{50}) is confirmed to be 750 mg/kg (in the 'Material Safety Data Sheet' provided by Sigma Aldrich, USA along with the drug).

One fruitful area of research could be to study the synergistic combination of suramin with other drugs. The synergistic combination of drugs (if proven successful) leads to the lowering of costs, reduction in dosage, enhancement in healing rates and reduces the emergence of resistant strains (when compared to monotherapy). Combination drug therapy with suramin and eflornithine or DFMO (DL- α -difluoromethylornithine) was found to be effective against acute (Stage II) *T. b. Rhodesiense* infection in murine models [50]. Previous work in our laboratory also noted the *in vitro* synergism between suramin and paromomycin [8] (which is currently used as an antileishmanial in the field). Thus, in conclusion there is a possibility that suramin could be included in the repertoire of antileishmanial drugs and could prove useful in a major outbreak of VL.

Supporting information

S1 Fig. Gel images of GAPDH, iNOS, Granzyme B, Perforin mRNA expressions. Gene expression levels of iNOS, Granzyme-B, Perforin and GAPDH were carried out in all the experimental groups of animals by semi quantitative RT-PCR analysis.

(TIF)

S2 Fig. Suramin effect on T cell populations. Effect of suramin on splenic CD4 $^+$ and CD8 $^+$ T cell populations was investigated by flow cytometry analysis in a BDLSR Fortessa analyser and respective percentages of CD4 $^+$ and CD8 $^+$ cells were determined using BD FACSDIVA software. The bar diagrams give the percentage of respective T cell in total splenocytes. Unpaired two-tailed Student's t-test was performed and levels of significance are indicated by P values. (TIF)

S1 Table. Primer sequences used for the present study. Semiquantitative RT PCR analysis was performed to investigate the iNOS, perforin, and granzyme B expression levels in all the experimental groups by using the respective forward and reverse primers.

(DOCX)

Acknowledgments

The authors gratefully acknowledge Dr.Nahid Ali (Indian Institute of Chemical Biology, Kolkata) for the kind gift of transformed AG83 parasite. We are grateful to Prof. ParthaSaha (Saha Institute of Nuclear Physics, Kolkata) for providing us with the infrastructure to perform some of the experiments and to Dr.SansaDutta (Saha Institute of Nuclear Physics, Kolkata), Aditya-Singha Roy (Saha Institute of Nuclear Physics, Kolkata), IndranilModak (Saha Institute of Nuclear Physics, Kolkata), Dr.SemantiGhosh(Saha Institute of Nuclear Physics, Kolkata), GargiBiswas(Saha Institute of Nuclear Physics, Kolkata), Dr. PrasantaSaini (Bose Institute, Kolkata)for theirvaluable inputs. Dr.Semantee Bhattacharya (Indian Association for the Cultivation of Science, Jadavpur, Kolkata 700032, India) is acknowledged for her kind help.Dr. SushantaDebnath (Saha Institute of Nuclear Physics, Kolkata), Mr. Saikat Mukherjee (Saha Institute of Nuclear Physics, Kolkata) are acknowledged for their technical support. We are thankful to Dr.Kuladip Jana (Bose Institute, Kolkata) for technical support in the animal model experiments.Mr Debasish Sen (Saha Institute of Nuclear Physics) has also given us invaluable technical support in the improvement of the figures.We also gratefully acknowledge the DBT-RA Program in Biotechnology and Life Sciences, Government of India,for the fellowship of SK.

Author Contributions

Conceptualization: Supriya Khanra, Subrata Majumdar, Rahul Banerjee.

Data curation: Supriya Khanra, Subir Kumar Juin, Junaid Jibran Jawed, Sweta Ghosh, Shreyasi Dutta, Shaik Abdul Nabi.

Formal analysis: Supriya Khanra, Dipak Dasgupta, Subrata Majumdar, Rahul Banerjee.

Investigation: Supriya Khanra, Subir Kumar Juin, Dipak Dasgupta, Subrata Majumdar, Rahul Banerjee.

Project administration: Subrata Majumdar, Rahul Banerjee.

Resources: Jyotirmayee Dash.

Supervision: Dipak Dasgupta, Subrata Majumdar, Rahul Banerjee.

Writing – original draft: Supriya Khanra, Rahul Banerjee.

Writing – review & editing: Supriya Khanra, Subrata Majumdar, Rahul Banerjee.

References

1. Alvar J, Yactayo S, Bern C. Leishmaniasis and poverty. *Trends Parasitol.* 2006; 22:552–7. <https://doi.org/10.1016/j.pt.2006.09.004> PMID: 17023215
2. Salotra P, Singh R. Challenges in the diagnosis of post kala-azar dermal leishmaniasis. *Indian J Med Res.* 2006; 123:295–310. PMID: 16778312
3. Bi K, Chen Y, Zhao S, Kuang Y, John Wu CH. Current Visceral Leishmaniasis Research: A Research Review to Inspire Future Study. *Biomed Res Int.* 2018; 2018:9872095. <https://doi.org/10.1155/2018/9872095> PMID: 30105272
4. Khanra S, Sarraf NR, Das S, Das AK, Roy S, Manna M. Genetic markers for antimony resistant clinical isolates differentiation from Indian Kala-azar. *Acta Trop.* 2016; 164:177–84. <https://doi.org/10.1016/j.actatropica.2016.09.012> PMID: 27629023
5. Purkait B, Kumar A, Nandi N, Sardar AH, Das S, Kumar S, et al. Mechanism of amphotericin B resistance in clinical isolates of *Leishmania donovani*. *Antimicrob Agents Chemother.* 2012; 56:1031–41. <https://doi.org/10.1128/AAC.00030-11> PMID: 22123699
6. Khanra S, Sarraf NR, Das AK, Roy S, Manna M. Miltefosine resistant field isolate from Indian kala-azar patient shows similar phenotype in experimental infection. *SciRep.* 2017; 7:10330.

7. Moore EM, Lockwood DN. Treatment of visceral leishmaniasis. *J Glob Infect Dis.* 2010; 2:151–8. <https://doi.org/10.4103/0974-777X.62883> PMID: 20606971
8. Khanra S, Kumar YP, Dash J, Banerjee R. In vitro screening of known drugs identified by scaffold hopping techniques shows promising leishmanicidal activity for suramin and netilmicin. *BMC Res Notes.* 2018; 11:319. <https://doi.org/10.1186/s13104-018-3446-y> PMID: 29784022
9. Misset O, Opperdoes FR. The phosphoglycerate kinases from *Trypanosoma brucei*. A comparison of the glycosomal and the cytosolic isoenzymes and their sensitivity towards suramin. *Eur J Biochem* 1987; 162:493–500. <https://doi.org/10.1111/j.1432-1033.1987.tb10667.x> PMID: 3830152
10. Albulescu IC, van Hoolwerff M, Wolters LA, Bottaro E, Nastruzzi C, Yang SC, et al. Suramin inhibits chikungunya virus replication through multiple mechanisms. *Antiviral Res.* 2015; 121:39–46. <https://doi.org/10.1016/j.antiviral.2015.06.013> PMID: 26112648
11. Henss L, Beck S, Weidner T, Biedenkopf N, Sliva K, Weber C, et al. Suramin is a potent inhibitor of Chikungunya and Ebola virus cell entry. *Virol J.* 2016; 13: 149–59. <https://doi.org/10.1186/s12985-016-0607-2> PMID: 27581733
12. Li H, Li H, Qu H, Zhao M, Yuan B, Cao M, et al. Suramin inhibits cell proliferation in ovarian and cervical cancer by downregulating heparanase expression. *Cancer Cell Int.* 2015; 15:52. <https://doi.org/10.1186/s12935-015-0196-y> PMID: 26052253
13. Ren P, Zou G, Bailly B, Xu S, Zeng M, Chen X, et al. The approved pediatric drug suramin identified as a clinical candidate for the treatment of EV71 infection—suramin inhibits EV71 infection in vitro and in vivo. *Emerg Microbes Infect.* 2014; 3:e62. <https://doi.org/10.1038/emi.2014.60> PMID: 26038755
14. Garcia AR, Oliveira DMP, Amaral ACF, Jesus JB, Rennó Sodero AC, Souza AMT, et al. *Leishmania infantum* arginase: biochemical characterization and inhibition by naturally occurring phenolic substances. *J Enzyme Inhib Med Chem.* 2019; 34:1100–09. <https://doi.org/10.1080/14756366.2019.1616182> PMID: 31124384
15. Mukherjee S, Mukherjee B, Mukhopadhyay R, Naskar K, Sundar S, Dujardin JC, et al. Imipramine is an orally active drug against both antimony sensitive and resistant *Leishmania donovani* clinical isolates in experimental infection. *PLoS Negl Trop Dis.* 2012; 6:e1987.
16. Das A, Das MC, Das N, Bhattacharjee S. Evaluation of the antileishmanial potency, toxicity and phytochemical constituents of methanol bark extract of *Sterculia villosa*. *Pharm Biol.* 2017; 55:998–1009. <https://doi.org/10.1080/13880209.2017.1285946> PMID: 28173714
17. Shimasaki H. Assay of fluorescent lipid peroxidation products. *Methods Enzymol.* 1994; 233:338–46.
18. Khanra S, Bandopadhyay SK, Chakraborty P, Datta S, Mondal D, Chatterjee M, et al. Characterization of the recent clinical isolates of Indian Kala-azar patients by RAPD-PCR method. *J Parasit Dis.* 2011; 35:116–22. <https://doi.org/10.1007/s12639-011-0048-1> PMID: 23024491
19. Shrivahare R, Vishwakarma P, Parmar N, Yadav PK, Haq W, Srivastava M, et al. Combination of liposomal CpGoligodeoxynucleotide2006 and miltefosine induces strong cell-mediated immunity during experimental visceral leishmaniasis. *PLoS One.* 2014; 9:e94596. <https://doi.org/10.1371/journal.pone.0094596> PMID: 24732039
20. Amin DN, Masocha W, Ngan'dwe K, Rottenberg M, Kristensson K. Suramin and minocycline treatment of experimental African trypanosomiasis at an early stage of parasite brain invasion. *Acta Trop.* 2008; 106: 72–4. <https://doi.org/10.1016/j.actatropica.2008.01.005> PMID: 18329619
21. Basu R, Bhaumik S, Basu JM, Naskar K, De T, Roy S. Kinetoplastid membrane protein-11 DNA vaccination induces complete protection against both pentavalent antimonial-sensitive and -resistant strains of *Leishmania donovani* that correlates with inducible nitric oxide synthase activity and IL-4 generation: evidence for mixed T_H1 and T_H2-like responses in visceral leishmaniasis. *J Immunol.* 2005; 174: 7160–71. <https://doi.org/10.4049/jimmunol.174.11.7160> PMID: 15905560
22. Stauber AL. Resistance to the Khartoum strain of *Leishmania donovani*. *Rice Inst Pamphlet.* 1956; 45: 80–96.
23. Datta S, Manna M, Khanra S, Ghosh M, Bhar R, Chakraborty A, et al. Therapeutic immunization with radio-attenuated *Leishmania* parasites through i.m. route revealed protection against the experimental murine visceral leishmaniasis. *Parasitol Res.* 2012; 111: 361–9. <https://doi.org/10.1007/s00436-012-2847-4> PMID: 22437790
24. Datta S, Khanra S, Chakraborty A, Roy S, Manna M. Evaluation of s.c. route of immunization by homologous radio attenuated live vaccine in experimental murine model of visceral leishmaniasis. *J Parasit Dis.* 2016; 40:436–43. <https://doi.org/10.1007/s12639-014-0522-7> PMID: 27413317
25. Chowdhury S, Mukherjee T, Mukhopadhyay R, Mukherjee B, Sengupta S, Chattopadhyay S, et al. The lignan niranthin poisons *Leishmania donovani* topoisomerase IB and favours a Th1 immune response in mice. *EMBO Mol Med.* 2012; 4:1126–43. <https://doi.org/10.1002/emmm.201201316> PMID: 23027614

26. Datta S, Adak R, Chakraborty P, Haldar AK, Bhattacharjee S, Chakraborty A, et al. Radioattenuated Leishmanial parasites as immunoprophylactic agent against experimental murine visceral leishmaniasis. *Exp Parasitol.* 2012; 130:39–47.
27. Misset O, Opperdoes FR. Simultaneous purification of hexokinase, class-I fructose-bisphosphate aldolase, triosephosphateisomerase and phosphoglyceratekinase from *Trypanosoma brucei*. *Eur J Biochem.* 1984; 144:475–83.
28. Eikmanns BJ. Identification, sequence analysis, and expression of a *Corynebacterium glutamicum* gene cluster encoding the three glycolytic enzymes glyceraldehyde-3-phosphate dehydrogenase, 3-phosphoglycerate kinase, and triosephosphateisomerase. *J Bacteriol.* 1992; 174:6076–86. <https://doi.org/10.1128/JB.174.19.6076-6086.1992> PMID: 1400158
29. Dutta S, Basak A, Dasgupta S. Design and synthesis of enediyne-peptide conjugates and their inhibiting activity against chymotrypsin. *Bioorg Med Chem.* 2009; 17: 3900–8. <https://doi.org/10.1016/j.bmc.2009.04.019> PMID: 19428261
30. Gautam S, Kumar R, Maurya R, Nylén S, Ansari N, Rai M, et al. IL-10 neutralization promotes parasite clearance in splenic aspirate cells from patients with visceral leishmaniasis. *J Infect Dis.* 2011; 204:1134–7. <https://doi.org/10.1093/infdis/jir461> PMID: 21881130
31. Want MY, Islammudin M, Chouhan G, Ozbak HA, Hemeg HA, Chattopadhyay AP, et al. Nanoliposomal artemisinin for the treatment of murine visceral leishmaniasis. *Int J Nanomedicine.* 2017; 12:2189–2204. <https://doi.org/10.2147/IJN.S106548> PMID: 28356736
32. Samant M, Gupta R, Kumari S, Misra P, Khare P, Kushawaha PK, et al. Immunization with the DNA-encoding N-Terminal domain of proteophosphoglycan of *Leishmania donovani* generates Th1-Type immunoprotective response against experimental visceral leishmaniasis. *J Immunol.* 2009; 183: 470–9. <https://doi.org/10.4049/jimmunol.0900265> PMID: 19542458
33. Morgan HP, McNae IW, Nowicki MW, Zhong W, Michels PA, Auld DS, et al. The trypanocidal drug suramin and other trypan blue mimetics are inhibitors of pyruvate kinases and bind to the adenosine site. *J Biol Chem.* 2011; 286:31232–40. <https://doi.org/10.1074/jbc.M110.212613> PMID: 21733839
34. Babokhov P, Sanyaolu AO, Oyibo WA, Fagbenro-Beyioku AF, Iriemenam NC. A current analysis of chemotherapy strategies for the treatment of human African trypanosomiasis. *Pathog Glob Health.* 2013; 107:242–52. <https://doi.org/10.1179/2047773213Y.0000000105> PMID: 23916333
35. Xu R, Pelicano H, Zhou Y, Carew JS, Feng L, Bhalla KN, et al. Inhibition of glycolysis in cancer cells: a novel strategy to overcome drug resistance associated with mitochondrial respiratory defect and hypoxia. *Cancer Res.* 2005; 65:613–21. PMID: 15695406
36. Sen N, Das BB, Ganguly A, Banerjee B, Sen T, Majumdar HK. *Leishmania donovani*: Intracellular ATP level regulates apoptosis-like death in luteolin induced dyskinetoplastid cells. *Exp Parasitol.* 2006; 114:204–14. <https://doi.org/10.1016/j.exppara.2006.03.013> PMID: 16707127
37. Shadab M, Jha B, Asad M, Deepthi M, Kamran M, Ali N. Apoptosis-like death in *Leishmania donovani* treated with KalsomeTM10, a new liposomal amphotericin B. *PLoS One* 2017; 12: e0171306. <https://doi.org/10.1371/journal.pone.0171306> PMID: 28170432
38. Carvalho L, Luque-Ortega JR, Manzano JI, Castanys S, Rivas L, Gamarro F. Tafenoquine, an anti-plasmodial 8-aminoquinoline, targets *Leishmania* respiratory complex III and induces apoptosis. *Antimicrob Agents Chemother.* 2010; 54:5344–51. <https://doi.org/10.1128/AAC.00790-10> PMID: 20837758
39. Lukheeram RV, Zour R, Varma AD, Xia B. CD4⁺T Cells: Differentiation and Functions. *Clin Dev Immunol.* 2012; 2012: 9251352012
40. Tripathi P, Singh V, Naik S. Immune response to Leishmania: paradox rather than paradigm. *FEMS Immunol Med Microbiol.* 2007; 51:229–42. <https://doi.org/10.1111/j.1574-695X.2007.00311.x> PMID: 17714488
41. Liu D, Uzonna JE. The early interaction of *Leishmania* with macrophages and dendritic cells and its influence on the host immune response. *Front Cell Infect Microbiol.* 2012; 2:83.
42. Mossmann TR, Coffman RL. TH1 and TH2 cells: different patterns of lymphokine secretion lead to different functional properties. *Ann Rev Immunol.* 1989; 7:145–73.
43. Kindt TJ, Goldsby RA, Osborne BA. *Kuby Immunology*. W.H. Freeman and Company, New York. 2007. pp 462.
44. Santos EC, Novaes RD, Cupertino MC, Bastos DSS, Klein RC, Silva EAM et al. Concomitant benznidazole and suramin chemotherapy in mice infected with a virulent strain of *Trypanosoma cruzi*. *Antimicrob Agents and Chemother.* 2015; 59:5999–6006.
45. Waterhouse NJ, Clarke CJP, Sedelies KA, Teng MW, Trapani JA. Cytotoxic lymphocytes: instigators of dramatic target cell death. *Biochemical Pharmacol.* 2004; 68:1033–40.
46. Voogd TE, Vansterkenburg EL, Wilting J, Janssen LH. Recent research on the biological activity of suramin. *Pharmacol Rev.* 1993; 45:177–203. PMID: 8396782

47. McGeary RP, Bennett AJ, Tran QB, Cosgrove KL, Ross BP. Suramin: clinical uses and structure-activity relationships. *Mini Rev Med Chem.* 2008; 8:1384–94. <https://doi.org/10.2174/138955708786369573> PMID: 18991754
48. Wilson M, Callens M, Kuntz DA, Perié J, Opperdoes FR. Synthesis and activity of inhibitors highly specific for the glycolytic enzymes *Trypanosoma brucei*. *Mol Biochem Parasitol.* 1993; 59:201–10.
49. Barrett MP, Boykin DW, Brun R, Tidwell RR. Human African trypanosomiasis: pharmacological re-engagement with a neglected disease. *Br J Pharmacol.* 2007; 152: 1155–71. <https://doi.org/10.1038/sj.bjp.0707354> PMID: 17618313
50. Bacchi CJ, Nathan HC, Yarlett N, Goldberg B, McCann PP, Sjoerdsma A, et al. Combination chemotherapy of drug-resistant *Trypanosoma brucei rhodesiense* infections in mice using DL-alphadifluoromethyl ornithine and standard trypanocides. *Antimicrob Agents Chemother.* 1994; 38:563–569. <https://doi.org/10.1128/aac.38.3.563> PMID: 8203855

UNCORRECTED PROOF